



ELSEVIER

SCIENCE @ DIRECT®

PHYSICS LETTERS B

Physics Letters B 589 (2004) 103–110

www.elsevier.com/locate/physletb

Search for neutrinoless decays $\tau \rightarrow 3\ell$

Belle Collaboration

Y. Yusa^{aj}, T. Nagamine^{aj}, A. Yamaguchi^{aj}, K. Abe^e, K. Abe^{ai}, T. Abe^e, I. Adachi^e,
 H. Aihara^{ak}, M. Akatsu^r, Y. Asano^{ao}, V. Aulchenko^a, T. Aushevⁱ, S. Bahinipati^c,
 A.M. Bakich^{af}, E. Banas^v, I. Bedny^a, U. Bitenc^j, I. Bizjak^j, A. Bondar^a, A. Bozek^v,
 M. Bračko^{p,j}, T.E. Browder^d, M.-C. Chang^u, B.G. Cheon^{ae}, R. Chistovⁱ, Y. Choi^{ae},
 A. Chuvikov^{ab}, M. Danilovⁱ, L.Y. Dong^g, S. Eidelman^a, V. Eigesⁱ, Y. Enari^r,
 S. Fratina^j, N. Gabyshev^e, A. Garmash^{ab}, T. Gershon^e, G. Gokhroo^{ag}, B. Golob^{o,j},
 J. Haba^e, H. Hayashii^s, M. Hazumi^e, L. Hinzⁿ, T. Hokuue^r, Y. Hoshi^{ai}, W.-S. Hou^u,
 T. Iijima^r, K. Inami^r, A. Ishikawa^e, R. Itoh^e, H. Iwasaki^e, M. Iwasaki^{ak}, J.H. Kang^{as},
 J.S. Kang^l, P. Kapusta^v, N. Katayama^e, H. Kawai^b, T. Kawasaki^x, H. Kichimi^e,
 H.O. Kim^{ae}, P. Koppenburg^e, S. Korpar^{p,j}, P. Križan^{o,j}, P. Krokovny^a, A. Kuzmin^a,
 Y.-J. Kwon^{as}, S.H. Lee^{ad}, T. Lesiak^v, J. Li^{ac}, S.-W. Lin^u, J. MacNaughton^h,
 T. Matsumoto^{am}, A. Matyja^v, Y. Mikami^{aj}, W. Mitaroff^h, H. Miyata^x, D. Mohapatra^{aq},
 G.R. Moloney^q, T. Mori^{al}, Y. Nagasaka^f, E. Nakano^y, M. Nakao^e, H. Nakazawa^e,
 Z. Natkaniec^v, S. Nishida^e, O. Nitoh^{an}, T. Nozaki^e, S. Ogawa^{ah}, T. Ohshima^r,
 T. Okabe^r, S. Okuno^k, S.L. Olsen^d, W. Ostrowicz^v, H. Ozaki^e, P. Pakhlovⁱ, H. Palka^v,
 H. Park^m, K.S. Park^{ae}, N. Parslow^{af}, J.-P. Perroudⁿ, L.E. Piilonen^{aq}, A. Poluektov^a,
 N. Root^a, H. Sagawa^e, S. Saitoh^e, Y. Sakai^e, T.R. Sarangi^{ap}, O. Schneiderⁿ,
 A.J. Schwartz^c, S. Semenovⁱ, K. Senyo^r, M.E. Sevior^q, H. Shibuya^{ah}, B. Shwartz^a,
 J.B. Singh^{aa}, N. Soni^{aa}, S. Stanič^{ao,l}, M. Starič^j, K. Sumisawa^z, T. Sumiyoshi^{am},
 S. Suzuki^{ar}, O. Tajima^{aj}, F. Takasaki^e, K. Tamai^e, N. Tamura^x, M. Tanaka^e,
 Y. Teramoto^y, T. Tomura^{ak}, T. Tsuboyama^e, T. Tsukamoto^e, S. Uehara^e, T. Uglovⁱ,
 Y. Unno^b, S. Uno^e, G. Varner^d, C.C. Wang^u, C.H. Wang^t, Y. Yamada^e, Y. Yamashita^w,
 M. Yamauchi^e, H. Yanai^x, J. Zhang^e, Z.P. Zhang^{ac}, V. Zhilich^a, T. Ziegler^{ab},
 D. Žontar^{o,j}

^a Budker Institute of Nuclear Physics, Novosibirsk, Russia

^b Chiba University, Chiba, Japan

^c University of Cincinnati, Cincinnati, OH, USA

^d University of Hawaii, Honolulu, HI, USA

^e High Energy Accelerator Research Organization (KEK), Tsukuba, Japan

^f Hiroshima Institute of Technology, Hiroshima, Japan

^g Institute of High Energy Physics, Chinese Academy of Sciences, Beijing, PR China

- ^h Institute of High Energy Physics, Vienna, Austria
ⁱ Institute for Theoretical and Experimental Physics, Moscow, Russia
^j J. Stefan Institute, Ljubljana, Slovenia
^k Kanagawa University, Yokohama, Japan
^l Korea University, Seoul, South Korea
^m Kyungpook National University, Taegu, South Korea
ⁿ Swiss Federal Institute of Technology of Lausanne, EPFL, Lausanne, Switzerland
^o University of Ljubljana, Ljubljana, Slovenia
^p University of Maribor, Maribor, Slovenia
^q University of Melbourne, Victoria, Australia
^r Nagoya University, Nagoya, Japan
^s Nara Women's University, Nara, Japan
^t National United University, Miao Li, Taiwan
^u Department of Physics, National Taiwan University, Taipei, Taiwan
^v H. Niewodniczanski Institute of Nuclear Physics, Krakow, Poland
^w Nihon Dental College, Niigata, Japan
^x Niigata University, Niigata, Japan
^y Osaka City University, Osaka, Japan
^z Osaka University, Osaka, Japan
^{aa} Panjab University, Chandigarh, India
^{ab} Princeton University, Princeton, NJ, USA
^{ac} University of Science and Technology of China, Hefei, PR China
^{ad} Seoul National University, Seoul, South Korea
^{ae} Sungkyunkwan University, Suwon, South Korea
^{af} University of Sydney, Sydney, NSW, Australia
^{ag} Tata Institute of Fundamental Research, Bombay, India
^{ah} Toho University, Funabashi, Japan
^{ai} Tohoku Gakuin University, Tagajo, Japan
^{aj} Tohoku University, Sendai, Japan
^{ak} Department of Physics, University of Tokyo, Tokyo, Japan
^{al} Tokyo Institute of Technology, Tokyo, Japan
^{am} Tokyo Metropolitan University, Tokyo, Japan
^{an} Tokyo University of Agriculture and Technology, Tokyo, Japan
^{ao} University of Tsukuba, Tsukuba, Japan
^{ap} Utkal University, Bhubaneswer, India
^{aq} Virginia Polytechnic Institute and State University, Blacksburg, VA, USA
^{ar} Yokkaichi University, Yokkaichi, Japan
^{as} Yonsei University, Seoul, South Korea

Received 27 March 2004; accepted 13 April 2004

Available online 23 April 2004

Editor: M. Doser

Abstract

We have searched for neutrinoless τ lepton decays into three charged leptons using an 87.1 fb^{-1} data sample collected with the Belle detector at the KEKB e^+e^- collider. Since the number of signal candidate events is compatible with that expected from the background, we set 90% confidence level upper limits on the branching fractions in the range $(1.9\text{--}3.5) \times 10^{-7}$ for various decay modes $\tau^- \rightarrow \ell^- \ell^+ \ell^-$ where ℓ represents e or μ .

© 2004 Published by Elsevier B.V. Open access under [CC BY license](#).

PACS: 13.35.Dx; 14.60.Fg; 11.30.Hv

Keywords: TAU lepton flavor violation

1. Introduction

In the Standard Model (SM), lepton-flavor-violating (LFV) decays of charged leptons are forbidden or highly suppressed even if neutrino mixing is taken into account [1]. LFV is expected in many extensions of the SM such as SUSY models with Higgs mediation [2], right-handed neutrinos [3,4], multi-Higgs bosons [5], extra Z' gauge bosons [6] and R -parity violating interactions [7]. Some of those models predict LFV decays of charged τ leptons enhanced to a level accessible at present B -factories. Observation of LFV would provide evidence for new physics beyond the SM.

In this Letter, we report on a search for six LFV τ decay modes: $\tau^- \rightarrow e^-e^+e^-$, $\tau^- \rightarrow e^-\mu^+\mu^-$, $\tau^- \rightarrow e^+\mu^-\mu^-$, $\tau^- \rightarrow \mu^-e^+e^-$, $\tau^- \rightarrow \mu^+e^-e^-$ and $\tau^- \rightarrow \mu^-\mu^+\mu^-$. Charge conjugate decay modes are implied throughout the Letter. Upper limits on the branching fractions for these decays at the level $(1-2) \times 10^{-6}$ at 90% confidence level have been set by the CLEO Collaboration using a data sample of 4.79 fb^{-1} [8]. Recently these results were improved on by the BaBar experiment which reported upper limits in the range $(1.1-3.3) \times 10^{-7}$ from a 91.5 fb^{-1} data sample [9]. We present here a new search based on a data sample of 87.1 fb^{-1} corresponding to (79.3 ± 1.1) million τ -pairs collected with the Belle detector [10] at the KEKB asymmetric energy e^+e^- collider [11] operating at a center-of-mass energy $\sqrt{s} \simeq 10.6 \text{ GeV}$.

2. Event selection

The Belle detector is a general purpose detector with excellent capabilities for precise vertex determination and particle identification. Tracking of charged particles is performed by a three-layer double-sided silicon vertex detector (SVD) and a fifty-layer cylindrical drift chamber (CDC) located in a 1.5 T magnetic field. Charged hadrons are identified by means of dE/dx from the CDC, signal pulse-heights from aerogel Čerenkov counters (ACC), and timing information from time-of-flight scintillation counters (TOF). Energies of photons are measured using a CsI (TI) electro-

magnetic calorimeter (ECL). Muons are detected by fourteen layers of resistive plate counters interleaved with iron plates (KLM).

We search for $\tau^+\tau^-$ events in which one τ decays into three charged leptons (3-prong) and the other τ decays into one charged and any number of neutrals (1-prong), which has a branching fraction of $(85.35 \pm 0.07)\%$ [12]. We start by requiring signal candidate events to have four charged tracks with zero net charge and any number of photons. Each charged track must have transverse momentum $p_t > 0.1 \text{ GeV}/c$ and be within the polar angle range $25^\circ < \theta < 140^\circ$. For each charged track, the distance of closest approach to the interaction point (IP) is required to be within $\pm 1 \text{ cm}$ transversely and $\pm 3 \text{ cm}$ along the beam. Photon candidates are selected from neutral ECL clusters with an energy $E_{\text{cluster}} > 0.1 \text{ GeV}$, where neutral ECL clusters must be separated by at least 30 cm from a projection point of any charged track in the ECL. The tracks and photons in an event are divided into two hemispheres in the e^+e^- center-of-mass system (CMS) by the plane perpendicular to the thrust axis calculated from the momenta of all charged tracks and photons in the event. Signal candidates have a 1-prong vs 3-prong topology, i.e., three charged tracks are required in one hemisphere, one charged track in the other. We define the former hemisphere as the signal side and the latter as the tag side. The number of photon candidates on the signal side, n_γ , should be less than or equal to two, to allow for photons from initial state radiation or photon radiation in the detector by electron tracks.

Electrons are identified by means of an electron likelihood function (\mathcal{L}_e), that includes the information on the dE/dx measurement in the CDC and the ratio of the cluster energy in the ECL to the track momentum measured in the CDC [13]. For electrons, we require $\mathcal{L}_e > 0.1$ and the laboratory momentum to be greater than $0.3 \text{ GeV}/c$. In order to correct for the energy loss from bremsstrahlung in the detector material, the momentum of an electron candidate is recalculated by adding the momentum of radiated photon clusters when an ECL cluster with energy less than 1.0 GeV is detected within a cone angle of 10° around the flight direction of the electron candidate track. The muon likelihood function (\mathcal{L}_μ) is evaluated from two variables—the difference between the range calculated from the momentum of a particle and the

E-mail address: yusa@awa.tohoku.ac.jp (Y. Yusa).

¹ On leave from Nova Gorica Polytechnic, Nova Gorica, Slovenia.

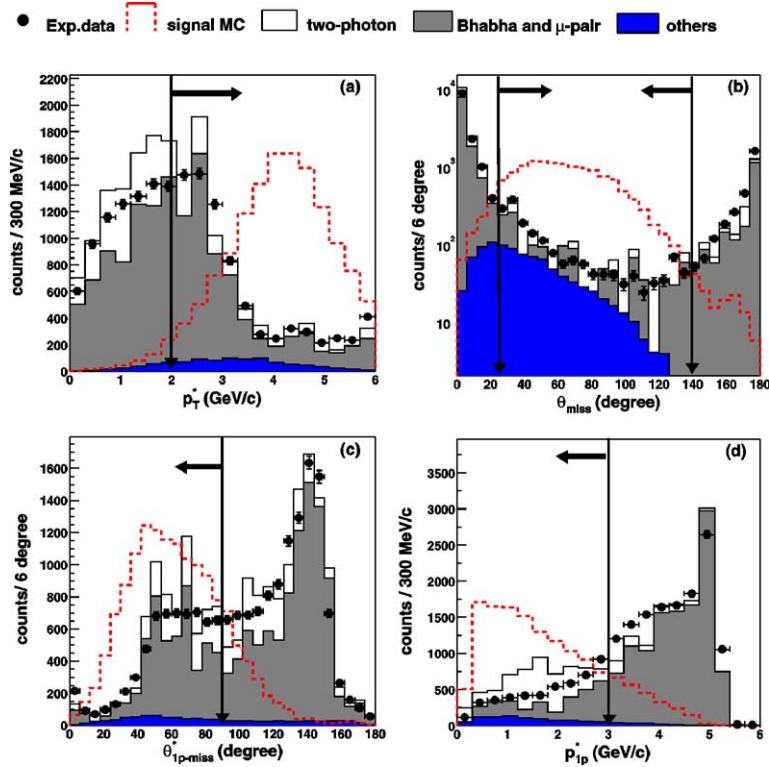


Fig. 1. Kinematical distributions used in the event selection after the event topology and lepton identification requirements: (a) the total transverse momentum p_T^* , (b) the polar angle of the missing momentum θ_{miss} , (c) the opening angle between the momentum of a 1-prong track and the missing momentum $\theta_{1p\text{-miss}}^*$, (d) the momentum of a 1-prong track p_{1p}^* . The distributions for experimental data, signal MC and background MC are indicated by closed circles, the dashed and solid histograms, respectively. The areas of the signal MC are normalized assuming a branching fraction of 1.3×10^{-3} while the background MC is normalized to the data luminosity. Background MC from two-photon, Bhabha and μ -pair, and other processes (generic $\tau\tau$, $e^+e^- \rightarrow q\bar{q}$ continuum and $B\bar{B}$ events, respectively) are shown by the open, shaded and dark histograms, respectively. The distributions are shown for the $\tau^- \rightarrow e^-e^+e^-$ mode. Although the size of each background source depends on the decay mode, the shape of each background is common to all. The shape of signal distributions is also similar for the six decay modes.

range measured in the KLM as well as the χ^2 value of the KLM hits with respect to the extrapolated track [14]. For muons, \mathcal{L}_μ is required to be larger than 0.1 and its momentum should be larger than 0.6 GeV/c. The requirement of lepton identification for all three charged tracks on the signal side leads to significant background reduction by a factor in the range from 10^2 to 10^4 for each decay mode with a 40% loss of signal.

For the Monte Carlo (MC) simulation of the signal, one τ lepton is assumed to decay into the signal LFV modes with a uniform phase space distribution in the τ rest frame and the other τ decays generically using the KORALB/TAUOLA program [15].

One important source of background remaining after requiring the event topology and lepton identifi-

cation on the signal side is due to radiative Bhabha events with a converted photon. This background is efficiently reduced by requiring that the invariant mass of any two oppositely charged particles be greater than $0.2 \text{ GeV}/c^2$, assuming the electron mass for each particle. The remaining background after removing photon conversions comes from two-photon processes, τ -pair events with generic decays into three charged hadrons, $e^+e^- \rightarrow q\bar{q}$ continuum and $B\bar{B}$ events, where hadrons are misidentified as leptons on the signal side.

For signal τ -pair events there is a missing momentum due to neutrino emission from the τ on the tag side. Fig. 1(a) shows the total transverse momentum p_T^* , the transverse component of the sum of momen-

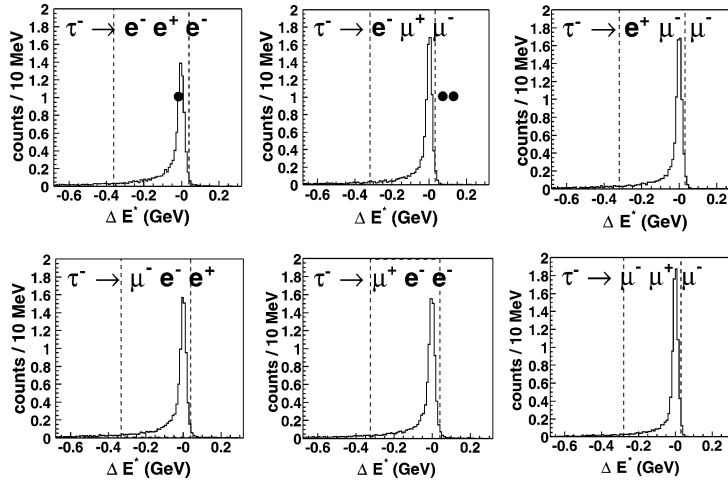


Fig. 2. ΔE^* distributions of the events in the ΔM signal region. Open histograms are the signal MC sample assuming the branching fraction of 1.3×10^{-6} , while experimental data is plotted by closed circles. The dashed lines indicate the ΔE^* signal region.

tum vectors for the four charged tracks in the CMS. To suppress events from two-photon processes, p_T^* is required to be larger than $2.0 \text{ GeV}/c$. We calculate the missing momentum by subtracting the momentum of all charged tracks and photons from the beam momentum. In order to suppress radiative Bhabha and two-photon events, the polar angle of the missing momentum in the laboratory frame θ_{miss} , must be between 25° and 140° , as shown in Fig. 1(b). The missing momentum due to neutrinos from the τ on the tag side tends to lie in the same hemisphere as the 1-prong track for signal events. The opening angle between the 1-prong track and missing momentum in the CMS, $\theta_{1\text{p-miss}}^*$, is required to be less than 90° , as shown in Fig. 1(c). Finally, the momentum of the 1-prong tag side track, $p_{1\text{p}}^*$, must be less than $3 \text{ GeV}/c$. Since the tag side τ decays with neutrino(s) or π^0 emission, the momentum of the 1-prong track is much smaller than the τ momentum. This requirement suppresses most of the Bhabha and μ -pair backgrounds, as shown in Fig. 1(d). After all these requirements, the background is reduced by a factor of order 10^4 with a 10% efficiency for the signal.

From the total CMS energy, $E_{3\ell}^*$, and invariant mass, $M_{3\ell}$, of the three signal side leptons, we compute the quantities: $\Delta E^* \equiv E_{3\ell}^* - E_{\text{beam}}^*$ and $\Delta M \equiv M_{3\ell} - M_\tau$, where E_{beam}^* is the CMS beam energy and M_τ is the τ mass. In the $\Delta E^* - \Delta M$ plane, the neutrinoless τ decay events are expected to be distributed

close to the origin. The ΔE^* and ΔM distributions for each decay mode are shown in Figs. 2 and 3, respectively, together with expectations based on signal MC. It is seen that each peak has a tail on the lower side that is due to initial state radiation or bremsstrahlung of a charged particle interacting with the detector material. Since electrons radiate more than muons, the shape of the peak depends on the decay mode.

The signal region for each decay mode is given in Table 1, and is illustrated as the region between two dashed lines in Figs. 2 and 3. Each signal region is defined to contain 90% of the signal MC events plotted in the figures. Fig. 4 shows the ΔE^* vs ΔM plot for the data. In the fourth and fifth columns of Table 1, we compare the number of events found for the data and the normalized MC background in the plotted region of $-0.68 \text{ GeV} < \Delta E^* < 0.32 \text{ GeV}$ and $-0.12 \text{ GeV}/c^2 < \Delta M < 0.12 \text{ GeV}/c^2$ shown in Fig. 4.

3. Results

Efficiencies for $\tau \rightarrow 3\ell$ decays with a uniform phase space distribution vary from 9.2% to 9.5% and are listed in the second column of Table 2. The actual decay angle distribution, however, will depend on the LFV interaction and include spin correlations between the tag side and signal side τ [16]. In order to

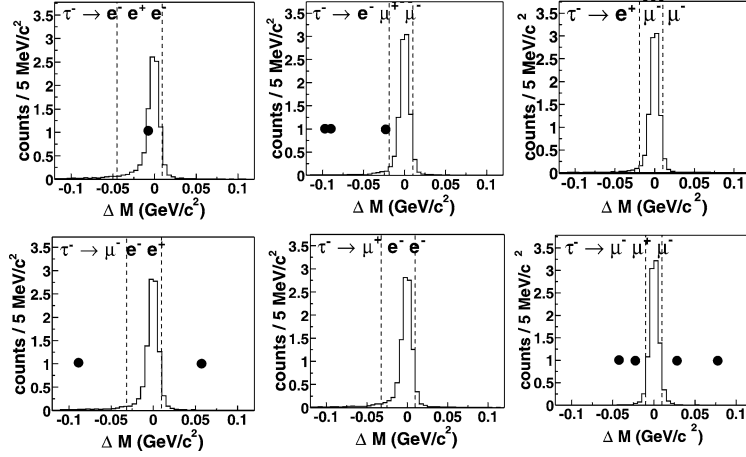


Fig. 3. ΔM distributions of the events in the ΔE^* signal region. Open histograms are the signal MC sample assuming the branching fraction of 1.3×10^{-6} , while experimental data is plotted by closed circles. The dashed lines indicate the ΔM signal region.

Table 1

Definition of the signal regions for each decay mode and the number of events in Fig. 4 for the data and the normalized background MC

Mode	Signal region		Number of events in the Fig. 4 area	
	ΔE^* (GeV)	ΔM (GeV/c ²)	Data	MC
$\tau^- \rightarrow e^- e^+ e^-$	$-0.36 < \Delta E^* < 0.04$	$-0.032 < \Delta M < 0.010$	1	0^{+17}_{-0}
$\tau^- \rightarrow e^- \mu^+ \mu^-$	$-0.32 < \Delta E^* < 0.03$	$-0.017 < \Delta M < 0.010$	18	5^{+17}_{-3}
$\tau^- \rightarrow e^+ \mu^- \mu^-$	$-0.32 < \Delta E^* < 0.03$	$-0.017 < \Delta M < 0.010$	0	2^{+3}_{-2}
$\tau^- \rightarrow \mu^- e^+ e^+$	$-0.33 < \Delta E^* < 0.04$	$-0.025 < \Delta M < 0.010$	2	0^{+3}_{-0}
$\tau^- \rightarrow \mu^+ e^- e^-$	$-0.33 < \Delta E^* < 0.04$	$-0.025 < \Delta M < 0.010$	0	0^{+3}_{-0}
$\tau^- \rightarrow \mu^- \mu^+ \mu^-$	$-0.28 < \Delta E^* < 0.03$	$-0.010 < \Delta M < 0.010$	5	8 ± 4

evaluate the maximum possible effect of such correlations, we examine $V - A$ and $V + A$ interactions using the formulae given in [16]. The relative differences in the efficiencies ($\Delta\epsilon/\epsilon$) from a uniform distribution are found to be -3.8% , -8.7% , -1.1% , $+0.8\%$, -12.6% and -5.6% for $\tau^- \rightarrow e^- e^+ e^-$, $\tau^- \rightarrow e^- \mu^+ \mu^-$, $\tau^- \rightarrow e^+ \mu^- \mu^-$, $\tau^- \rightarrow \mu^- e^+ e^+$, $\tau^- \rightarrow \mu^+ e^- e^-$ and $\tau^- \rightarrow \mu^- \mu^+ \mu^-$ decay mode, respectively. Requirements on the number of CDC tracks and the energy of ECL clusters that are used to detect τ -pair events also constitute part of the trigger logic. The impact of the trigger on the efficiency is investigated by applying a trigger simulation to the signal MC. The changes in the detection efficiencies are found to be only a few percent, because the selection criteria applied in this analysis are much more restrictive than the trigger conditions.

As shown in Fig. 4, the background level in and around the signal region is very low. From the background MC, we find that the remaining events are due to the low-multiplicity $e^+ e^- \rightarrow q\bar{q}$ continuum or $B\bar{B}$ events where final-state hadrons are misidentified as leptons as well as a few events from generic τ -pair decay. As seen from Table 1, the numbers of events found in the Fig. 4 area are consistent with the numbers expected from the normalized background MC.

To evaluate the background b in the signal region, we assume a uniform background distribution along the ΔM axis in Fig. 4. With looser selection criteria, we find the ΔM distribution is uniform. We estimate the number of background events in the signal region from the number of events observed in the dotted box, the ΔM side-band regions in Fig. 4. The systematic

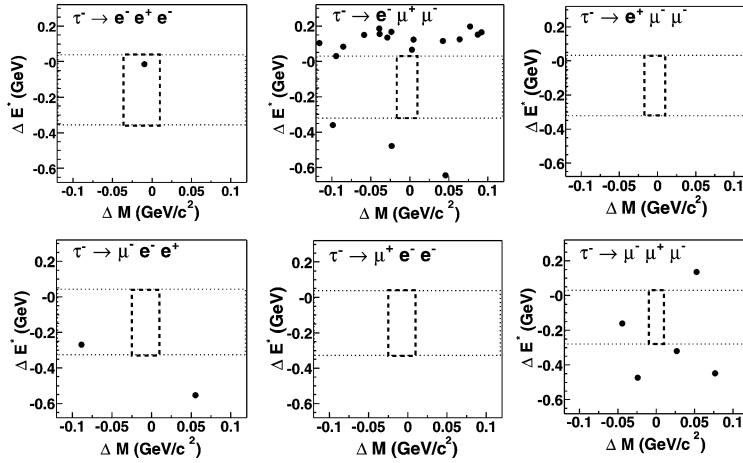


Fig. 4. ΔE^* vs ΔM plots for the experimental data. The charge conjugate decay mode is also included. The dashed and dotted boxes indicate the signal and ΔM side-band regions, respectively.

Table 2

Summary of detection efficiency, number of observed events, background expectation, s_0 and 90% C.L. upper limits on the branching fractions

Decay mode	Detection efficiency ϵ (%)	Number of events observed	Expected background b	Upper limit of \mathcal{B} $\times 10^{-7}$	
				s_0	
$\tau^- \rightarrow e^- e^+ e^-$	9.2 ± 0.6	1	< 0.2	4.36	3.5
$\tau^- \rightarrow e^- \mu^+ \mu^-$	9.2 ± 1.4	0	0.1 ± 0.1	2.54	2.0
$\tau^- \rightarrow e^+ \mu^- \mu^-$	9.2 ± 1.1	0	< 0.3	2.55	2.0
$\tau^- \rightarrow \mu^- e^- e^+$	9.4 ± 0.8	0	0.2 ± 0.2	2.49	1.9
$\tau^- \rightarrow \mu^+ e^- e^-$	9.5 ± 1.4	0	< 0.2	2.55	2.0
$\tau^- \rightarrow \mu^- \mu^+ \mu^-$	9.0 ± 1.6	0	0.1 ± 0.1	2.51	2.0

uncertainty for this method is estimated by comparing the observed and estimated number of events in the region outside of the dotted box in Fig. 4. The fourth column of Table 2 shows the number of estimated background events and its error, including both systematic and statistical uncertainties.

In the signal regions for the six decay modes considered, one candidate is observed for the $\tau^- \rightarrow e^- e^+ e^-$ mode while no candidates are found for the other modes. The numbers of events in the signal regions are consistent with the background expectations.

We determine the upper limit s_0 on the number of signal events at 90% CL using the prescription of Feldman and Cousins [17]. To include in this limit the uncertainty in the detection efficiency ϵ , we increase s_0 according to the prescription of Cousins and Highland [18]. The main systematic uncertainties in the detection efficiencies come from tracking (1.0% per track),

electron identification (1.1% per electron), muon identification (5.4% per muon), trigger efficiency (1.4%), statistics of signal MC (1.0%) and uncertainty of the decay angular distribution (0.8–12.6%). The total uncertainty of the detection efficiency is 6.1% for $\tau^- \rightarrow e^- e^+ e^-$, 15.1% for $\tau^- \rightarrow e^- \mu^+ \mu^-$, 12.4% for $\tau^- \rightarrow e^+ \mu^- \mu^-$, 8.4% for $\tau^- \rightarrow \mu^- e^- e^+$, 15.1% for $\tau^- \rightarrow \mu^+ e^- e^-$ and 17.5% for $\tau^- \rightarrow \mu^- \mu^+ \mu^-$ mode. The uncertainty in the number of τ -pair events comes from the luminosity measurement (1.4%). For our calculation of s_0 , we take the background (and its uncertainty) to be zero. This results in conservative upper limits. Upper limits for branching fractions \mathcal{B} are calculated for each decay mode as follows: $\mathcal{B}(\tau^- \rightarrow l^- l^+ l^-) < \frac{s_0}{2N_{\tau\tau} \times \epsilon \times \mathcal{B}_1}$, where $N_{\tau\tau}$ is the total number of the τ -pairs produced, and \mathcal{B}_1 is the inclusive 1-prong branching fraction of the τ . The values of s_0 used and the resulting upper lim-

its for the branching fractions are summarized in Table 2.

4. Summary

We have searched for lepton-flavor-violating decays $\tau^- \rightarrow \ell^- \ell^+ \ell^-$ using an 87.1 fb^{-1} data sample. No evidence for any of these decay modes is observed and upper limits for the branching fractions are obtained in the range $(1.9\text{--}3.5) \times 10^{-7}$ for $\tau^- \rightarrow \ell^- \ell^+ \ell^-$ modes; these are approximately one order of magnitude more restrictive than the limits previously obtained by CLEO [8] and comparable to the recent results from BaBar [9].

Acknowledgements

We wish to thank the KEKB accelerator group for the excellent operation of the KEKB accelerator. We acknowledge support from the Ministry of Education, Culture, Sports, Science, and Technology of Japan and the Japan Society for the Promotion of Science; the Australian Research Council and the Australian Department of Education, Science and Training; the National Science Foundation of China under contract No. 10175071; the Department of Science and Technology of India; the BK21 program of the Ministry of Education of Korea and the CHEP SRC program of the Korea Science and Engineering Foundation; the Polish State Committee for Scientific Research under contract No. 2P03B 01324; the Ministry of Science and Technology of the Russian Federation; the Ministry of Education, Science and Sport of the Republic of Slovenia; the National Science Council and the Ministry of Education of Taiwan; and the US Department of Energy.

References

- [1] W.J. Marciano, A.I. Sanda, Phys. Lett. B 67 (1977) 303; B.W. Lee, R.E. Shrock, Phys. Rev. D 16 (1977) 1444; T.P. Cheng, L.F. Li, Phys. Rev. D 16 (1977) 1425.
- [2] K.S. Babu, C. Kolda, Phys. Rev. Lett. 89 (2002) 241802; A. Dedes, J. Ellis, M. Raidal, Phys. Lett. B 549 (2002) 159.
- [3] J.R. Ellis, et al., Phys. Rev. D 66 (2002) 115013.
- [4] F. Borzumati, A. Masiero, Phys. Rev. Lett. 57 (1986) 961; J. Hisano, T. Moroi, K. Tobe, M. Yamaguchi, T. Yanagida, Phys. Lett. B 357 (1995) 579; J. Hisano, T. Moroi, K. Tobe, M. Yamaguchi, Phys. Rev. D 53 (1996) 2442; J. Hisano, D. Nomura, Phys. Rev. D 59 (1999) 116005.
- [5] E. Ma, Phys. Rev. D 64 (2001) 097302; E. Ma, M. Raidal, U. Sarkar, Phys. Rev. Lett. 85 (2000) 3769; E. Ma, Phys. Rev. D 66 (2002) 037301.
- [6] C. Yue, Y. Zhang, L. Liu, Phys. Lett. B 547 (2002) 252.
- [7] J.E. Kim, P. Ko, D. Lee, Phys. Rev. D 56 (1997) 100.
- [8] D.W. Bliss, et al., CLEO Collaboration, Phys. Rev. D 57 (1998) 5903.
- [9] B. Aubert, et al., BaBar Collaboration, Phys. Rev. Lett. 92 (2004) 121801.
- [10] A. Abashian, et al., Belle Collaboration, Nucl. Instrum. Methods A 479 (2002) 117.
- [11] S. Kurokawa, E. Kikutani, Nucl. Instrum. Methods A 499 (2003) 1, and other papers included in this volume.
- [12] K. Hagiwara, et al., Phys. Rev. D 66 (2002) 010001.
- [13] K. Hanagaki, et al., Nucl. Instrum. Methods A 485 (2002) 490.
- [14] A. Abashian, et al., Nucl. Instrum. Methods A 491 (2002) 69.
- [15] KORALB(v2.4)/TAUOLA(v2.6); S. Jadach, Z. Wąs, Comput. Phys. Commun. 85 (1995) 453; S. Jadach, Z. Wąs, Comput. Phys. Commun. 64 (1991) 267; S. Jadach, Z. Wąs, R. Decker, J.H. Kühn, Comput. Phys. Commun. 76 (1993) 361; S. Jadach, Z. Wąs, R. Decker, J.H. Kühn, Comput. Phys. Commun. 70 (1992) 69; S. Jadach, Z. Wąs, R. Decker, J.H. Kühn, Comput. Phys. Commun. 64 (1991) 275.
- [16] R. Kitano, Y. Okada, Phys. Rev. D 63 (2001) 113003.
- [17] G.J. Feldman, R.D. Cousins, Phys. Rev. D 57 (1998) 3873.
- [18] R.D. Cousins, V.L. Highland, Nucl. Instrum. Methods A 320 (1992) 331.